APPENDIX 6

EASYSPIN: SIMULATING CW ESR SPECTRA

Stefan Stoll and Arthur Schweiger
Physical Chemistry Laboratory, ETH Hönggerberg,
Zürich, Switzerland

1. INTRODUCTION

Only the simplest of cw ESR spectra, those with few, sharp, well-resolved and sufficiently intense lines, can be analyzed in a straightforward manner. The magnetic parameters of the paramagnetic species can directly be obtained from line positions, amplitudes, and widths using simple analytical formulae. However, such formulae do not exist for all cases. Often, physical information is implicit and hidden in the details of the line shape. It is not always possible to assign lines, especially in spectra from molecules with many magnetic nuclei. When several interactions are of similar strength, line positions and intensities behave in a nontrivial manner. A straightforward analysis by read-out may also be impeded by high spectral noise levels and by very broad or strongly overlapping lines.

Thus, for many cw ESR spectra, a full-scale quantum-theoretical numerical simulation, possibly combined with least-squares fitting, is necessary to reproduce the spectrum and to recover the underlying structural and dynamic parameters. Spectral simulation is therefore an important ingredient of the successful application of ESR spectroscopy.

In this overview, we describe EasySpin, a software package that is able to simulate cw ESR spectra of most paramagnetic systems under a wide range of dynamic conditions. EasySpin is a collection of functions and programs intended to run on Matlab, a commercial software platform for technical and scientific computation and visualization, available for several operating systems (Windows, Linux, and others). EasySpin 2.5 is included on the CD accompanying the book, and that version is also the one referred to and used in this overview. The latest version is available from www.easyspin.ethz.ch.

This overview summarizes the core concepts of the ESR simulation algorithms implemented in EasySpin. Full details can be found in Stoll and Schweiger (2006) and the references cited therein, as well as in the EasySpin documentation included on the CD. Many of the examples in this overview are related to simple nitroxide radicals, as often applied in membrane biophysics, but the programs in EasySpin can handle complex paramagnetic molecules with several unpaired electrons and several magnetic nuclei.

The Matlab code for all simulated spectra shown in this overview is included in the text. The code snippets should be almost self-explanatory to readers who are familiar with the basics of Matlab.

2. FOUR DYNAMIC REGIMES IN CW ESR

All the static ESR spectroscopic properties of a paramagnetic molecule are determined by the strengths and geometries of the interactions between the various magnetic moments present. For a molecule with one unpaired electron, these include the *g* tensor of the electron, its hyperfine couplings to nearby magnetic nuclei, their magnetogyric ratios, and their nuclear quadrupole tensors. For systems with more than one unpaired electron, couplings between the electrons are present as well.

All static interactions are to some extent anisotropic. They consist of an isotropic, orientation-independent part and a part that depends on the orientation of the paramagnetic molecule with respect to the spectrometer with its fixed magnetic field direction. Thus, a cw ESR spectrum is in general orientation-dependent: the resonance lines shift if the molecule is rotated.

The appearance of the ESR spectrum does not only depend on static interactions in the paramagnetic molecule, but on dynamic processes on the timescale of the ESR experiment as well. This ESR timescale is determined by the spectral anisotropy, $\Delta\omega$, i.e., the maximum difference between resonance line positions when the orientation of the molecule is varied. Any dynamic process that is not extremely slow ("frozen") on this timescale will affect the shape of the ESR spectrum.

The most important and most visible dynamic process in solutions or membranes observable by ESR is the tumbling of molecules. This rotational motion modulates the resonance frequencies and gives rise to fluctuating local magnetic fields that induce transitions. The rotational diffusional motion is a random process, and its timescale is characterized by rotational correlation time τ_c, denoting the characteristic time after which molecules with initially identical orientations lose their alignment.

By comparing the speed of the rotational diffusion (τ_c^{-1}) to the spectral anisotropy ($\Delta\omega$), we can distinguish four dynamic regimes with distinct types of ESR spectra: (1) isotropic limit, (2) fast motion, (3) slow motion, and (4) rigid limit. They are illustrated in Figure 1, together with sample spectra of a nitroxide radical.

In the *isotropic limit*, paramagnetic molecules are tumbling extremely fast, so that any anisotropic property is completely averaged out. Only the isotropic parts of all interactions are observable, that is, the isotropic *g* factor and the isotropic hyperfine coupling constants. The spectrum consists of a series of symmetric lines with equal widths. This is the case, for example, for many organic radicals in low-viscosity solutions at room temperature.

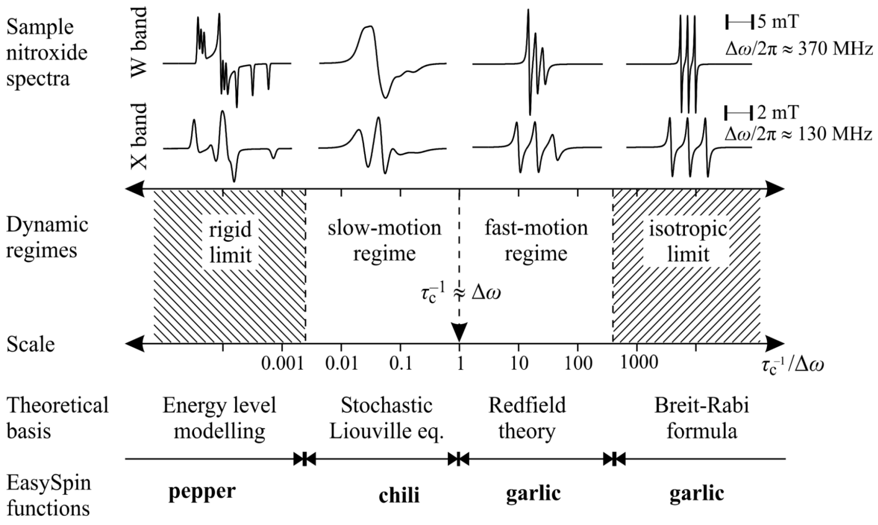

Figure 1. Schematic representation of the timescale of rotational dynamics accessible by cw ESR. τ_c: isotropic rotational correlation time, $\Delta\omega$: spectral anisotropy. The borders between the four regimes are only approximate. For each regime, representative X- and W-band cw ESR spectra of a nitroxide radical are shown.

At the other end of the range, in the *rigid limit*, the paramagnetic molecules are immobilized. There is neither translational nor rotational motion. The ESR spectra reveal the full anisotropy of all interactions. This is generally the case in powder materials, glasses, and frozen solutions at low temperatures.

Between these two extremes, there are dynamic regimes where the rotational motion is visibly affecting the spectrum but is too slow to completely average the anisotropic interactions. In the *fast-motion regime*, the rotational motion is fast enough so that the spectrum still appears similar to an isotropic-limit spectrum, although with line widths varying substantially from line to line.

In the *slow-motion regime*, the rotational diffusion is slower, so that the spectrum loses its similarity to the isotropic limiting case. The lines broaden and distort in an intuitively not easily understandable way. As the rotational motion slows down further, the spectrum successively approaches its rigid-limit shape.

The terms “slow” and “fast” do not refer to the absolute speed of reorientation, but are understood relative to the spectral broadening. Hence, a “fast” motion at the X band may become a “slow” motion at high spectrometer frequencies. Note that the borders between the four regimes in Figure 1 are not sharp. They also depend on the type of experiment: saturation-transfer ESR can detect movements in systems that appear completely “frozen” in a cw ESR experiment.

3. SIMULATION OF CW ESR SPECTRA

For the four dynamic regimes, different theoretical approaches and, consequently, different algorithms are used to simulate the resulting cw ESR spectra. All of them compute line positions, intensities, and widths before the spectrum is constructed. However, depending on the regime, various simplifications can be made. In the rigid and isotropic limits, rotational dynamics can be entirely ignored. In the fast-motion regime, the rotational diffusion can be treated as a small perturbation affecting only line widths. Only in the slow-motion regime is a full quantum-dynamical treatment necessary. In the following, we present each of the four regimes and their associated algorithms, including some illustrative simulations using EasySpin.

3.1. Isotropic limit

The simulation of cw ESR spectra of paramagnetic centers that tumble fast enough to completely average out all anisotropic interactions is simple. Spectral line intensities and widths are identical for all transitions. There are two methods for computing the line positions. Usually the hyperfine couplings are much smaller than the electron Zeeman splitting. Therefore, for a long time, the method of choice was based on explicit formulae for the energy levels obtained from perturbation theory:

$$E(m_\mathrm{S}, m_\mathrm{I}) \approx g_\mathrm{iso}\mu_\mathrm{B} m_\mathrm{S} B_0 + E^{(1)} + E^{(2)} + E^{(3)} + \cdots,$$
$$E^{(1)} = a_\mathrm{iso} m_\mathrm{S} m_\mathrm{I}, \qquad E^{(2)} = a_\mathrm{iso}^2 \frac{I(I+1) - m_\mathrm{I}^2}{2 g_\mathrm{iso}\mu_\mathrm{B} B_0},$$

where the first term in the sum is the electron Zeeman splitting, followed by perturbational correction terms of increasing order for the hyperfine splitting. To obtain the resonance line positions, the above expressions are inserted into resonance condition

$$E(+\tfrac{1}{2}, m_\mathrm{I}) - E(-\tfrac{1}{2}, m_\mathrm{I}) = h\nu_\mathrm{mw}\,,$$

which is then solved for B_0. For order n, this involves solution of a polynomial of degree n. For small hyperfine couplings, an evaluation to second order is sufficient to obtain accurate resonance fields. The convergence, though, can be very slow for large hyperfine couplings. To achieve convergence, high orders have to be incorporated.

There is a second, more general and more accurate way to obtain the resonance fields (Stoll et al. 2006). The isotropic spin Hamiltonian of a system with an unpaired electron and one nucleus with arbitrary spin can be diagonalized analytically, even for a large hyperfine coupling. The resulting energy levels as a function of the magnetic field are given by the Breit-Rabi formulae (Weil 1971). It is not possible to rearrange the resonance condition with these expressions to obtain an explicit solution for the resonance field, but numerically, a few fixed-point iterations based on

$$B_{k+1}(m_{\mathrm{I}}) = \frac{h a_{\mathrm{iso}}}{\gamma\left(1-\xi_k^2\right)}\left\{-m_{\mathrm{I}} \pm \sqrt{m_{\mathrm{I}}^2 + \left(1-\xi_k^2\right)\left[(2\xi_k)^{-2} - \left(I+\tfrac{1}{2}\right)^2\right]}\right\},$$

$$\xi_k = \frac{a_{\mathrm{iso}}/2}{\nu_{\mathrm{mw}} + \mu_{\mathbf{n}} g_{\mathrm{n}} B_k / h}, \qquad \gamma = \mu_{\mathrm{B}} g_{\mathrm{iso}} + \mu_{\mathrm{n}} g_{\mathrm{n}}$$

can solve the equation quickly. An excellent starting B_0 value is obtained by setting g_{n} to zero. Numerically, this method is very efficient: after two to four iterations, the value of B_k converges to the exact resonance field within numerical accuracy (i.e., 10^{-16} relative), even for hyperfine couplings almost as large as the electron Zeeman interaction.

In EasySpin, isotropic-limit spectra are computed by the function **garlic**, which implements this second approach. The following Matlab code simulates the isotropic spectrum of a nitroxide radical as shown in Figure 2a:

```
Nitroxide = struct('g', 2.0059, 'Nucs', '14N', 'A', 40, 'lw', [0.1, 0.15]);
XBand = struct('mwFreq', 9.5, 'CenterSweep', [338.4, 8]);
[B,spc] = garlic(Nitroxide,XBand);
```

The first line defines the nitroxide radical parameters. The *g* value, the nuclear isotope, the *A* value (in MHz), and the line width (in mT) are given. Here, the line width is specified to be a Lorentzian broadening with an FWHM (full width at half maximum) of 0.1 mT, convoluted with a Gaussian one with an FWHM of 0.15 mT. This way, the effect on the line shapes of unresolved hyperfine splittings, e.g., from protons, is easily accounted for. Experimental conditions are listed in the second line: the microwave frequency (in GHz) and the magnetic field range in terms of the center field and the sweep width (both in mT). The third line calls **garlic**, the EasySpin function that simulates the spectrum. The magnetic field axis and the spectrum are returned in B and spc, respectively.

garlic also works for more complicated radicals with several magnetic nuclei. The following code computes the solution spectrum of the anthracene radical anion. The resulting spectrum is shown in Figure 2b:

```
A = mt2mhz([-0.5337, -0.2740, -0.1509], gfree);
Anthracene = struct('g', gfree, 'Nucs', '1H,1H,1H', 'n', [2, 4, 4], 'A', A, 'lw', 0.02);
Params = struct('mwFreq', 9.6, 'nPoints', 16384);
[B,spc] = garlic(Anthracene,Params);
```

Often, hyperfine couplings of radicals are given in magnetic field units. In the first line, they are converted from mT to MHz using **mt2mhz**, a utility function of EasySpin. The second line defines the spin system. There are three types of protons. For each proton type, the hyperfine coupling and the equivalence number are given. The remaining lines are similar to those of the nitroxide example. Note that the field range is not specified: in this case, **garlic** determines it automatically.

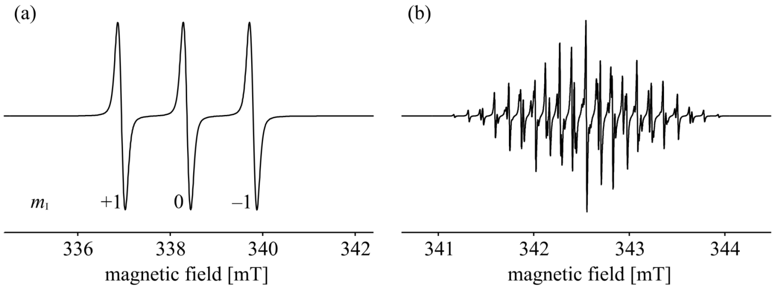

Figure 2. Isotropic cw ESR spectra simulated with EasySpin: (**a**) a generic nitroxide radical, (**b**) the anthracene radical anion. All simulation parameters are given in Matlab code in the text.

In such many-nuclei systems, **garlic** treats each group of equivalent nuclei separately and then combines the results in a first-order manner, neglecting any effect of one group of nuclei on the others. However, if one nucleus has a sufficiently large hyperfine coupling that it strongly influences the unpaired electron, it will also affect other nuclei via the electron. These indirect nuclear–nuclear cross-effects are neglected by **garlic**. In such cases, the rigid-limit algorithm described in §3.4 should be used. It is accurate for any number of nuclei and any magnitude of the hyperfine couplings, though much slower.

3.2. Fast-Motion Regime

If, starting from the very fast tumbling in the isotropic limit, the rotation of the paramagnetic molecules is slowed down either by cooling or by increasing the viscosity of the solvent, we enter the fast-motion regime. The spectral lines do not shift, and their shapes are still Lorentzian (possibly with a Gaussian contribution due to unresolved hyperfine couplings), but their widths increase relative to the isotropic limiting case. This broadening depends on the nuclear magnetic quantum numbers m_I and is thus different for each line.

In this fast-motion regime, the tumbling can be treated as a small perturbation, as long as the spectral anisotropy is small compared to the microwave frequency. The theory (Redfield theory) leads to practical expressions for the line widths. For the case of one nucleus with small hyperfine coupling, they are given by the quadratic formula (see, e.g., Atherton 1993)

$$\frac{1}{T_2} = A_0 + A + Bm_I + Cm_I^2 ,$$

where $1/(\pi T_2)$ is the FWHM of the Lorentzian line in the frequency domain. The terms with coefficients A, B, and C describe the broadening contribution from the rotational motion, whereas the first term, A_0, collects all other broadening effects.

With accurately known g and A tensors, the isotropic rotational correlation time τ_c can be obtained from A, B, and C according to

$$A = \frac{\mu_e^2}{h^2} B_0^2 (\Delta \boldsymbol{g}{:}\Delta \boldsymbol{g})\left[\tfrac{2}{15} j_0 + \tfrac{1}{10} j_1\right] + I(I+1)(\Delta \boldsymbol{A}{:}\Delta \boldsymbol{A})\left[\tfrac{2}{15} j_0 + \tfrac{7}{60} j_1\right],$$

$$B = \frac{16\pi^2}{15}\frac{\mu_e}{h} B_0 (\Delta \boldsymbol{g}{:}\Delta \boldsymbol{A})\left[\tfrac{5}{15} j_0 + \tfrac{1}{5} j_1\right],$$

$$C = (\Delta \boldsymbol{A}{:}\Delta \boldsymbol{A})\left[\tfrac{1}{12} j_0 - \tfrac{1}{60} j_1\right],$$

with spectral densities $j_0 = \tau_c$ and $j_1 = \tau_c/(1+\omega_0^2\tau_c^2)$. $\Delta\boldsymbol{g}$ and $\Delta\boldsymbol{A}$ are the anisotropic parts of the g and A tensors, i.e., $\Delta\boldsymbol{g} = \boldsymbol{g} - g_{\mathrm{iso}}\mathbf{1}$ and $\Delta\boldsymbol{A} = \boldsymbol{A} - a_{\mathrm{iso}}\mathbf{1}$. ($\Delta\boldsymbol{A}$ is assumed to be given in frequency units). The symbol $\boldsymbol{X}{:}\boldsymbol{Y}$ indicates element-by-element multiplication of the matrices followed by summation, giving a number characterizing the corresponding anisotropy.

From the formulae we see that the line widths are affected by both anisotropic hyperfine coupling $\Delta\boldsymbol{A}$ and g shift $\Delta\boldsymbol{g}$. Coefficients A and B are a function of magnetic field B_0, and, as a consequence, a larger magnetic field leads to larger values for A and B. The broadenings for a given molecule are thus different at different spectrometer frequencies. This is illustrated in Figure 3.

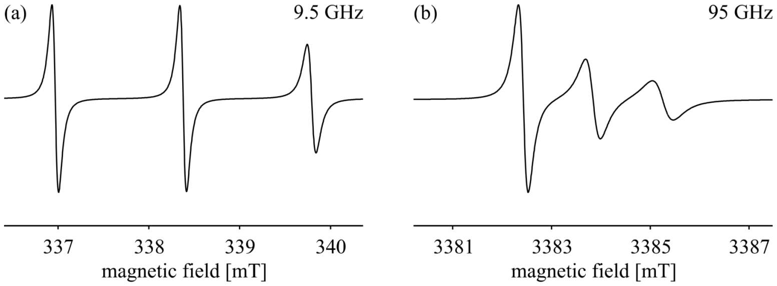

Figure 3. Fast-motion examples: (**a**) a generic nitroxide radical at 9.5 GH, (**b**) the same nitroxide radical at 95 GHz. All simulation parameters are given in Matlab code in the text.

EasySpin's simulation algorithm for the fast-motion regime is identical to the one used for isotropic spectra, with the only difference that each spectral line is constructed with a different line width according to the expressions given above. Only the isotropic rotational correlation time needs to be supplied to the function **garlic**, which then computes the line widths and builds the spectrum. In the following is the code for a nitroxide radical spectrum, with a rotational correlation time of 1 ns:

```
A = mt2mhz([5.8, 5.8, 30.8]/10);
Sys = struct('g', [2.0088, 2.0061, 2.0027], 'Nucs', '14N', 'A', A, 'lw', 0.1);
Sys.tcorr = 1e-9;
Exp = struct('mwFreq', 9.5);
[B, spc] = garlic(Sys, Exp);
```

The resulting spectrum is shown in Figure 3a.

Note that here, in contrast to the isotropic limit, **garlic** has to be given the full anisotropic *g* and *A* tensors in terms of their principal values, since they are needed to compute the line width parameters.

If we go from the X to W band by changing the spectrometer frequency in the above code to 95 GHz, but leaving the correlation time untouched, the line widths change significantly (see Figure 3b), as is expected due to their dependence on the magnetic field: The spectral anisotropy increases, the ESR timescale shrinks, and the same rotational motion is now "slower" relative to it.

Naturally, this method is not limited to nitroxide radicals. e.g., the fast-motion spectra of vanadyl or copper complexes can be computed by setting the corresponding isotope and changing the numerical values of *g* and *A* in the above code.

For paramagnetic molecules in which the unpaired electron interacts with more than one nucleus, the broadenings are not a simple sum over all nuclei of the quadratic line width formula. Cross-terms between the hyperfine anisotropies of different nuclei have to be added (Atherton 1993). **garlic** can handle this many-nuclei case. A simulation example, for the radical anion of p-fluoronitrobenzene, is shown in Figure 4. The code used contains full tensor information for all nuclei:

```
A_N = 40.40 + [24, -12, -12]; A_F = 22.51 + [34.9, -19.8, -15];
A_oH = [1, 1, 1]*9.69; A_mH = [1, 1, 1]*3.16;
Sys = struct('g', [2.0032, 2.0012, 2.0097], 'lw', 0.01);
Sys.Nucs = '14N,19F,1H,1H,1H,1H';
Sys.A = [A_N; A_F; A_oH; A_oH; A_mH; A_mH];
Sys.tcorr = 8e-11*2*pi;
Exp = struct('mwFreq', 9.5, 'nPoints', 1e4);
[B, spec] = garlic(Sys, Exp);
```

3.3. Slow-Motion Regime

When the rotational motion of the paramagnetic molecules slows down further, we leave the fast-motion regime and enter the slow-motion regime. The symmetric Lorentzian lines broaden substantially, become asymmetric, distort, and gradually converge to rigid-limit powder line shapes, revealing the full anisotropy of the underlying magnetic interactions (see the sample spectra in Figure 1).

The theory necessary to compute cw ESR spectra in this slow-motion regime is rather complicated. A full exposition of all aspects can be found in (Gamliel and Levanon 1995). The theory was developed and implemented by Freed and coworkers in a well-known program (Schneider and Freed 1989). We will shortly summarize the main aspects of the theory, as EasySpin's slow-motion simulation algorithm is based on it.

The central equation is the stochastic Liouville equation (SLE)

$$\frac{\partial}{\partial t}\rho(\boldsymbol{\Omega},t) = -\mathrm{i}[H(\boldsymbol{\Omega}(t)),\rho(\boldsymbol{\Omega},t)] - \Gamma_{\Omega}\left[\rho(\boldsymbol{\Omega},t) - \rho_0(\boldsymbol{\Omega})\right],$$

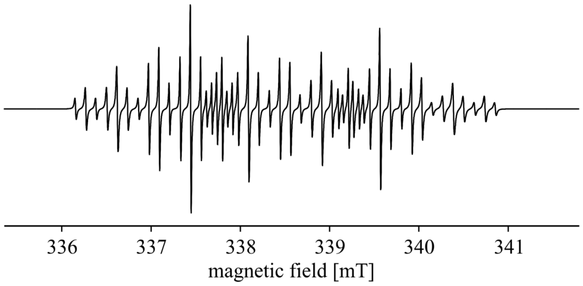

Figure 4. Fast-motion spectrum of the para-fluoronitrobenzene radical anion. All simulation parameters are given in Matlab code in the text.

which describes the time dependence of density matrix ρ in terms of spin Hamiltonian *H* and diffusion superoperator Γ_Ω. ρ_0 is the density matrix at thermal equilibrium, and all quantities depend on orientation $\boldsymbol{\Omega}$.

The SLE can be recast into a simpler form:

$$\frac{\partial}{\partial t}\chi(\boldsymbol{\Omega},t) = -\left[\mathrm{i}H^{\times}(\boldsymbol{\Omega}(t)) + \Gamma_\Omega\right]\chi(\boldsymbol{\Omega},t) = -L(\boldsymbol{\Omega},t)\chi(\boldsymbol{\Omega},t)\ ,$$

with out-of-equilibrium density $\chi = \rho - \rho_0$, Hamiltonian commutation superoperator H^x, and stochastic Liouville superoperator *L*, a shorthand notation for the term in square brackets. The absorption signal measurable in a cw ESR experiment is given by

$$I(\Delta\omega) \propto \mathrm{Re}(\boldsymbol{v}^{\dagger}\boldsymbol{u}) \quad \text{with} \quad \left(L + \mathrm{i}\Delta\omega\right)\boldsymbol{u} = \boldsymbol{v}\ ,$$

where ***v*** is the supervector describing the *x* magnetization, and Δω is the frequency offset from the center of the spectrum. In numerical simulations, superoperators are represented by matrices, and supervectors by column vectors.

The diffusion matrix Γ_Ω depends on the exact model for the rotational motion. The most common is rotational Brownian diffusion, analogous to translational Brownian motion. Other models include jump diffusion (the molecule is at rest for a certain time and the jumps instantaneously to another orientation) and free diffusion (the molecule is at rest for a certain time and the rotates directly and unimpeded to another orientation).

In contrast to the isotropic limit and the fast-motion regime, we are dealing with orientation-dependent quantities H^x, Γ_Ω, and ***v***. How can this orientation dependence be represented? The orientations are best described by three Euler angles, and the orientational distribution could be modeled using discrete orientations as basis functions. It is better, though, to use Wigner rotation functions $D^L{}_{KM}(\boldsymbol{\Omega})$, where $L \geq 0$ and $-L \leq K, M \leq L$. These functions are perfectly suited for the description, since they are the eigenfunctions of the rotational diffusion operator.

Each of these functions describes a continuous orientational distribution; by linear combinations any distribution can be modeled. Rotation functions for some values of *L*, *K*, and *M* are illustrated in Figure 5. (EasySpin's function **spherharm** was used to compute the plots.) The higher the parameters *L*, *K*, and *M*, the stronger the functions oscillate.

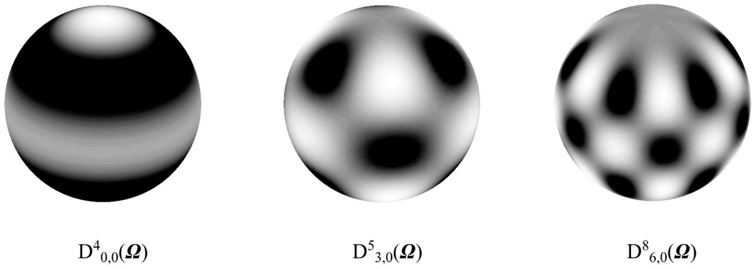

$D^{4}_{0,0}(\boldsymbol{\Omega})$ $D^{5}_{3,0}(\boldsymbol{\Omega})$ $D^{8}_{6,0}(\boldsymbol{\Omega})$

Figure 5. Illustration of rotational basis functions. Black (white) corresponds to negative (positive) values. The depicted functions have $M = 0$ und thus depend only on two of the three Euler angles describing the orientation of the paramagnetic molecule.

In general, a given orientational distribution is represented by a linear combination of an infinite number of such rotational basis functions. This is of course impractical, and the basis size is usually truncated to a finite number *N* of functions by specifying maximum values for *L*, *K*, and *M*. These values are chosen so that the error introduced is acceptable. The degree of truncation has to be determined by trial and error and depends on the speed of rotational diffusion and on the diffusion model used. If too few orientational basis functions are used, the spectrum will exhibit oscillating noise, just as in the case of the rigid-limit spectra described in §3.4.

For each possible rotation function, all ESR transitions involved in the dynamic process are included in the computation. For a nitroxide radical, this includes three allowed transitions as well as several forbidden ones, giving a total of, say, *P*. The total number of basis functions for representation of the Hamiltonian and the diffusion operators in matrix form is thus *PN*. The larger *P* and *N*, the larger the matrices.

The overall simulation procedure for slow-motional ESR spectra is schematically shown in Figure 6. It consists of three steps. First, matrices H^{x} and Γ and vector $\boldsymbol{v}$ are constructed in the basis described above. Then matrix $L= iH^{x} + \Gamma$ is reduced to tridiagonal form, using appropriate transformation algorithms. In these, vector $\boldsymbol{v}$ is used as a "starting vector." In the last step, each point in the spectrum is computed by evaluating a continued fraction expression containing the nonzero elements of the tridiagonal matrix.

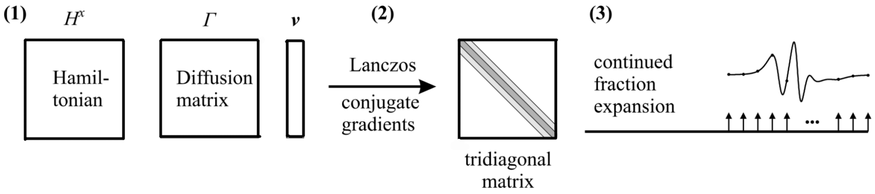

Figure 6. Illustration of the algorithm for solving the SLE: (1) H^x, Γ, and $\boldsymbol{v}$ are constructed in an appropriate basis, (2) matrix L is tri-diagonalised, (3) the tridiagonal matrix is used to compute the spectrum.

In EasySpin, the above algorithm for solving the SLE is implemented in the function **chili**. A simple simulation of a slow-motional ESR spectrum of a nitroxide radical, assuming Brownian rotational diffusion with an isotropic diffusion tensor, is shown in Figure 7a. The corresponding Matlab code is

```
Sys = struct('g', [2.008, 2.0061, 2.0027], 'Nucs', '14N', 'A', [16, 16, 86]);
Exp = struct('mwFreq',9.8);
Dynamics = struct('lw', 0.01, 'tcorr', 32e-9);
[x, spc] = chili(Sys, Exp, Dynamics);
```

The input is similar to that for the fast-motion regime. In the third line, all dynamic parameters are collected into a new structure, given as the third input argument to the function. In the above example, only the isotropic rotational correlation time and a residual line width are given. **chili** also supports an axial rotational diffusion tensor.

To rerun the simulation with another value for the rotational correlation time, two lines are sufficient:

```
Dynamics.tcorr = 100e-9;
[x, spc] = chili(Sys, Exp, Dynamics);
```

The spectrum depicted in Figure 7b is obtained.

If the hyperfine splittings from two or more nuclei are visible in the ESR spectrum, the simulation in the slow-motion regime gets more difficult, since the number of transitions, the dimensions of the matrices, and, consequently, the computation times increase tremendously — e.g., including another ^{14}N nucleus increases the matrix dimension by a factor of nine, giving 81 times more matrix elements.

Often, however, the spectral anisotropy is governed almost entirely by the anisotropy of the g tensor and of the hyperfine coupling of one nucleus only, and the hyperfine anisotropies of the other nuclei can be neglected. Then an approximative two-step technique can be used: the slow-motion spectrum is computed for the system with the first nucleus only. The hyperfine splitting pattern due to the other nuclei is accounted for by convoluting the slow-motion spectrum with a simple isotropic-limit stick spectrum due to all others. This post-convolution technique (Della Lunga et al. 1994) is implemented in **chili**. To simulate the slow-motional spectra of a planar Cu^{2+} complex, the following code is used. The main difference to the nitroxide example of Figure 7 is that now five nuclei (one ^{63}Cu and four ^{14}N) are included:

```
CuPc = struct('g', [2.0525, 2.0525, 2.1994], 'Nucs', '63Cu,14N', 'n', [1, 4]);
CuPc.A = [-54, -54, -608; 52.4, 41.2, 41.8];
Exp = struct('mwFreq', 9.878, 'Range', [260, 380]);
Dynamics.tcorr = 10^-7.35;
Dynamics.lw = 3;
Opt.LLKM = [14, 0, 0, 4];
[x, spc] = chili(CuPc, Exp, Dynamics, Opt);
```

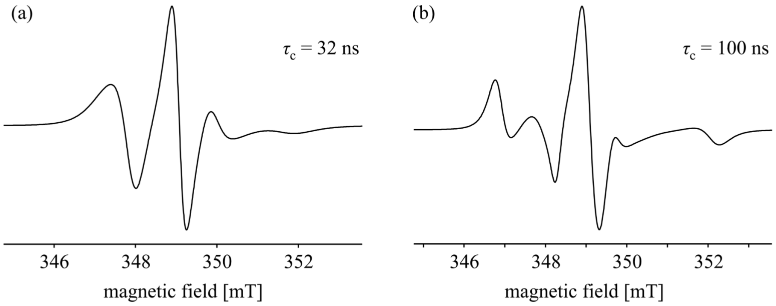

Figure 7. Two slow-motion examples of a generic nitroxide radical with isotropic Brownian rotational diffusion. All simulation parameters are given in Matlab code in the text.

The resulting spectrum is shown in Figure 8. The sixth line contains an explicit specification of the orientational basis size by giving maximum values for odd *L*, and even *L*, *K*, and *M*. Usually, however, **chili** chooses a reasonable basis size internally.

3.4. Rigid Limit

In the rigid limit, the paramagnetic molecules in the sample are fixed, and their orientations do not change with time. In crystals, only one or at most a few orientations are present, whereas in a powder, a glass, or a frozen solution all orientations occur with equal probability. As for the isotropic-limit and the fast-motion regime, the simulation of rigid-limit spectra entails two steps: the first positions, intensities, and widths of all resonance lines are computed for each orientation. In the second step, the total spectrum is constructed from this line information by summation or an equivalent procedure.

The following contains only an outline of the basics of EasySpin's computation of rigid-limit cw ESR line positions, intensities, and widths and the efficient procedure used to obtain the spectrum from these. More details can be found in Stoll et al. (2006) and the references cited therein.

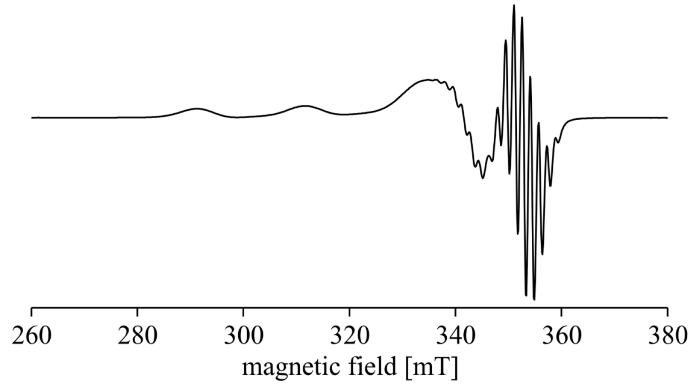

Figure 8. Slow-motion spectrum of Cu^{2+} phthalocyanine. All simulation parameters are given in Matlab code in the text.

To compute the resonance field positions for a given orientation of the paramagnetic molecule, various methods are commonly employed. For spin systems with hyperfine couplings and zero-field splittings small compared to the Zeeman splitting, explicit analytical formulae based on second-order perturbation theory can be used. EasySpin uses another much more general method (Stoll et al. 2003), which adaptively models the energy level diagram, from which the positions of resonance lines are then obtained.

The adaptive modeling of the energy levels as a function of the magnetic field works as follows (see Figure 9). First the energy levels at the left and right ends of the requested field range are computed by diagonalizing the associated spin Hamiltonians, giving the left and right ends of the diagram. Next, the levels at the center of the range are computed, yielding another set of energies. These are then compared to the approximate values obtained by cubic spline interpolation between the values at both ends of the range. If the interpolated and the exact energies are sufficiently close, the procedure terminates. If not, exact energies at the centers of the left and right half of the range are computed and then compared to values obtained by interpolation from the left and right ends of these segments. The algorithm works iteratively: any segment where the center modeling error is not small enough is subdivided further. The subdivisions continue until all segments are accurately modeled, resulting in a faithful cubic spline representation of the energy level diagram. Resonance positions for a given microwave frequency are readily obtained by searching though all the segments and solving the associated cubic equation if a resonance is possible.

This iterative segmentation method automatically adapts the number of field positions where energy levels are computed to the complexity of the energy level diagram. For simple systems only three diagonalizations are necessary, whereas in complex situations more than 50 can occur. Figure 9 illustrates this.

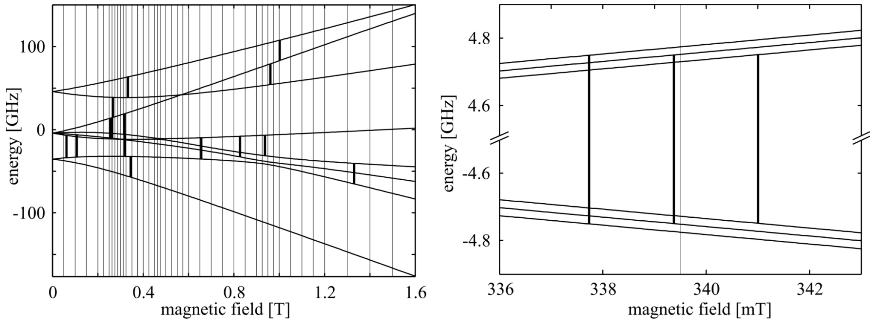

Figure 9. Energy level diagrams, resonances, and diagonalization positions of the iterative segmentation approach. (**a**) Tb^{4+} in ThO_2 ($S = 7/2$), 25 GHz (**b**) a generic nitroxide radical, 9.5 GHz

After the line positions, line intensities are computed. For a given transition between two energy levels, they are products of three factors: the ESR transition probability, the polarization term, and a frequency/field conversion factor.

The ESR transition probability is the modulus-square of the transition matrix element connecting the two energy levels. For nitroxide radicals, this probability is identical for all three allowed ESR transitions. However, for more complicated systems such as the one shown in Figure 9a, it can vary substantially from line to line.

The polarization term accounts for the fact that the line intensity is proportional to the population difference of the two levels involved in the transition. The populations can be in thermal (Boltzmann) equilibrium, or they can deviate from it due to a chemical or physical preparation process.

A frequency/field conversion factor is included since cw ESR spectra are not acquired as a function of the microwave frequency at constant magnetic field, but rather as a function of the magnetic field given constant microwave frequency. To obtain correct spectra, line intensities and line widths have to be multiplied by the difference of the inverse slopes of the energy levels involved. For simple systems, this factor is $1/g$.

Next come the line widths. Often, they are anisotropic due to the presence of many small and unresolved hyperfine couplings. Their orientation dependence is modeled by using a phenomenological anisotropic line width "tensor."

Another origin of anisotropic line widths are random static variations of the molecular structure around the unpaired electron, resulting in small distributions of the principal values of the interaction tensors (so-called g and A strain). In EasySpin simulations, these distributions are assumed to be Gaussian, and the dependence of the resonance line position on them is approximated as linear.

Both types of broadening give orientation-dependent line widths in frequency units. To convert them to magnetic field units, they have to be multiplied by the frequency/field conversion factor, as already discussed for line intensities.

In the next step, the ESR spectrum is constructed from the positions, intensities, and widths of all transitions. For single crystals, this is done by simply summing over all lines using Gaussian or Lorentzian line shapes for each of them. For disordered systems (powders, glasses, frozen solutions), these spectra have to be summed over all contributing orientations. The more orientations are included in this summation, the closer the total spectrum approximates the real spectrum, where more than 10^{11} molecules are usually contributing. If not enough orientations are included, the spectrum shows oscillating artefacts, so-called simulation noise.

First, a relatively small set of almost uniformly distributed orientations is set up by a very simple procedure. This is shown in Figure 10. Each orientation in this set is taken as a representative of all orientations that lie in its immediate neighborhood, which is called its Voronoi cell (see Figure 10). The area of the Voronoi cell (or a good estimate of it) is then used as a weight for the orientation's contribution to the powder spectrum.

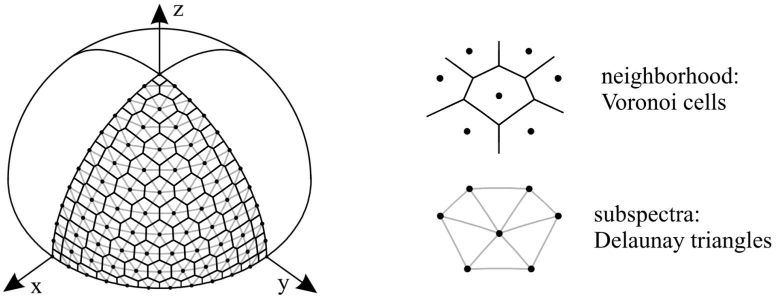

Figure 10. A simple spherical grid over one octant. Orientations are shown as dots; Voronoi cells and Delaunay triangles are indicated as well.

This weighted-sum-of-orientations approach is far from optimal: for small intrinsic line widths and large spectral anisotropies, thousands of orientations have to be evaluated and added. There exists a more efficient method, used in EasySpin, that automatically takes advantage of the anisotropy of the spectrum. Three neighboring orientations form the vertices of a small spherical triangular region, called a Delaunay triangle (see Figure 10). If the triangle is small enough, the total spectrum due to all orientations lying in it has a simple triangular shape, as shown in Figure 11. By constructing these subspectra for all Delaunay triangles and summing them up, the total powder spectrum is obtained (Stoll et al. 2006). This way, between 50 and 500 orientations per octant are sufficient for most simulations.

In EasySpin, the rigid-limit cw ESR spectra are computed by the function **pepper**. Its usage is similar to the one of **garlic** in the fast-motion regime. A rigid-limit powder ESR spectrum of a generic nitroxide radical is shown in Figure 12a. The necessary code is

```
Sys = struct('g', [2.008, 2.0061, 2.0027], 'Nucs', '14N', 'A', [16, 16, 86]);
Sys.lw = 0.1;
Exp = struct('mwFreq', 9.5, 'Range', [334 344]);
[B, spc] = pepper(Sys, Exp);
```

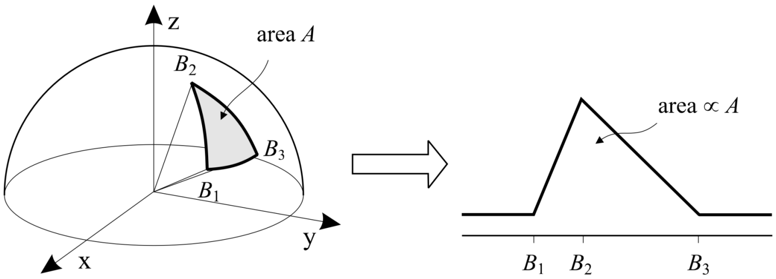

triangular set of orientations

triangular subspectrum

Figure 11. The set of orientations from a small spherical Delaunay triangle (left) give a powder subspectrum in the form of a triangle (right). B_1, B_2, and B_3 indicate resonance fields for the orientations corresponding to vertices of the spherical triangle.

It is not necessary to specify the number of orientations, which is a mandatory user-supplied parameter in many other powder cw ESR simulation programs. For most common systems, **pepper** is able to automatically choose this parameter to yield a smooth spectrum.

Instead of the entire powder spectrum, **pepper** can return one powder subspectrum for each ESR transition. This is demonstrated in Figure 12b. The following lines generate the group of spectra:

```
Sys = struct('g', [2.008, 2.0061, 2.0027], 'Nucs', '14N', 'A', [16, 16, 86]);
Sys.lw = 0.1;
Exp = struct('mwFreq', 9.5, 'Range', [334 344], ‘Harmonic’, 0);
Opt = struct(‘Output’, ‘separate’);
[B, spcs] = pepper(Sys, Exp, Opt);
```

In the fourth line, it is specified that **pepper** should return each transition in a separate spectrum. For demonstration, the harmonic is set to zero in the third line.

An example of a transition metal complex is shown in Figure 13a. Instead of a single well-defined hyperfine coupling, the simulation includes a distribution of A values (A strain), as specified via AStr and AStrain in the second and third lines. In addition, an anisotropic line width to model unresolved hyperfine splittings is specified by res and HStrain in the first and third line:

```
g = [2.28, 2.19, 2.01]; res =[1 1 1]*60;
A = [70, 30, 309]; AStr = [45, 25, 40];
Sys = struct('S', 1/2, 'Nucs', '59Co', 'g', g, 'A', A, 'AStrain', AStr, 'HStrain', res);
Exp = struct('Range', [261, 411], 'mwFreq', 9.475);
Opt = struct('Output', 'separate');
[B, specs, Transitions] = pepper(Sys, Exp, Opt);
```

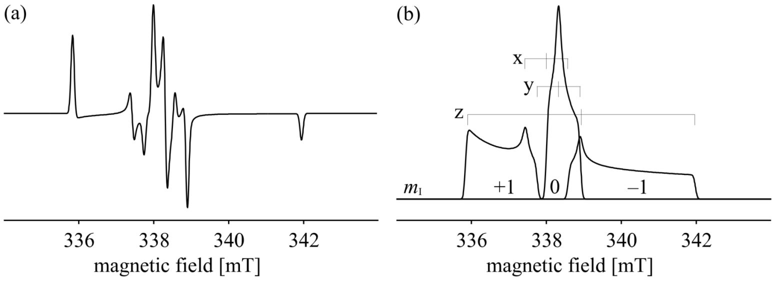

Figure 12. Powder cw ESR spectra of a generic nitroxide radical: (**a**) first-derivative spectrum, (**b**) absorption spectrum, separate transitions. All simulation parameters are given in Matlab code in the text.

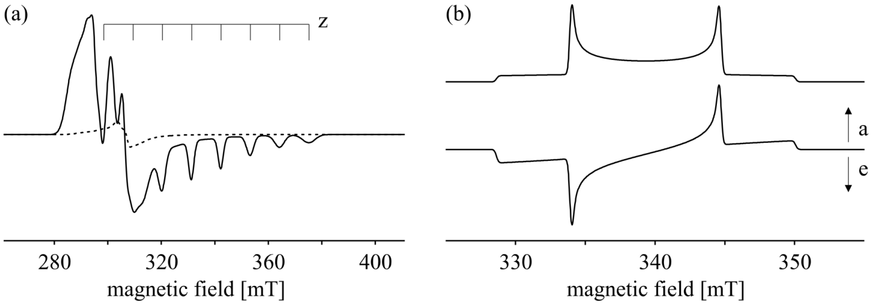

Figure 13. Powder cw ESR spectra simulated with **pepper**. (**a**) Co^{2+} complex including distributions of *A* values. The dashed spectrum represents the contribution of the forbidden ESR transitions. (**b**) A triplet state in thermal equilibrium (top) and with nonequilibrium populations of the three levels (bottom). All simulation parameters are given in Matlab code in the text.

Again, the simulation function was asked to return the simulated spectrum transition by transition. In the figure, the contributions from the forbidden transitions are shown separately. As a consequence of the *A* strain, the hyperfine lines in the high field region exhibit m_I-dependent broadenings. As mentioned above, in contrast to the fast-motion regime, these asymmetric broadenings are due to static distributions, and not to dynamic processes.

pepper can handle molecules with several unpaired electrons and several magnetic nuclei. High-order interaction terms for the electron spins are implemented. The simulation of spectra in oriented phases such as liquid crystals and membranes is supported by including appropriate weight factors during the summation of subspectra. Nonequilibrium populations are also possible: a sample simulation of the cw ESR spectrum of a molecule in an exited triplet state is

```
Sys = struct('S', 1, 'g', [2, 2, 2], 'lw', 0.3, 'D', [-1, -1, 2]*100);
Exp = struct('mwFreq', 9.5, 'Harmonic', 0, 'CenterSweep', [340, 30]);
Exp.Temperature = 298;
[B, spc1] = pepper(Sys, Exp);
Exp.Temperature = [0.85, 1, 0.95];
[B, spc2] = pepper(Sys, Exp);
```

In the third line, a temperature in Kelvin is given. In the fifth line, the same field is used to specify a nonequilibrium population vector for the zero-field states. The resulting two spectra are shown in Figure 13b.

5. OTHER EASYSPIN FUNCTIONS

Aside from the modules for simulating cw ESR spectra, EasySpin contains functions for a variety of ESR-related tasks. A list of all functions is included at the end of this overview. Here, we shortly focus on a few of them.

5.1. ENDOR Spectra

salt is an EasySpin function for simulating rigid-limit ENDOR spectra. Both disordered systems and single crystals are supported. The algorithm is very similar to that used for rigid-limit ESR spectra: The powder averaging is identical to the one in **pepper**, only the computation of line positions, intensities, and widths is different.

The ENDOR line positions of a nucleus in a paramagnetic molecule depend on its Larmor frequency and on its hyperfine coupling to the unpaired electron. Via the electron, it can feel the presence of other, strongly coupled nuclei, resulting in second-order line shifts. In addition, the nuclear quadrupole interaction can strongly affect the line positions. All these effects are accurately treated by **salt**, as it relies on a numerical computation of the energy levels by diagonalizing the spin Hamiltonian. Since the external magnetic field is kept constant in ENDOR experiments, the energy levels have to be computed only once for each orientation of the paramagnetic molecule. This makes the computation of powder ENDOR spectra much faster compared to the cw ESR case described above.

For each ENDOR transition, the line intensity is the product of three terms: (1) the ENDOR transition rate, which includes the hyperfine enhancement, (2) a factor giving the polarization of the transition, and (3) a selectivity factor taking into account that the only ENDOR transitions observed are those where one level is also involved in the ESR transition that is saturated. More details about the formulae implemented in **salt** can be found in Stoll et al. (2006).

5.2. Pulse ESR Spectra

Although EasySpin currently does not include a black-box function for the simulation of pulse ESR spectra, it provides various tools to support the necessary time-dependent simulations based on the density matrix formalism. The most important function is **evolve**, which evolves a given density matrix under a given Hamiltonian over a certain time. Both time-dependent and time-independent Hamiltonians are possible. **evolve** supports various pulse sequences.

5.3. Other Tools

levels and **levelsplot** are functions for computing and plotting energy level diagrams. The plot in Figure 9a was generated by **levelsplot**:

```
TbSys = struct('S', 7/2, 'g', [1, 1, 1]*2.0136);
b = -2527.53/60; c = -24.84/1260;
TbSys.B40 = b; TbSys.B44 = [5*b, 0];
TbSys.B60 = c; TbSys.B64 = [-21*c, 0];
levelsplot(TbSys, [1; 1]*pi/50, [0, 1600], 25);
```

Gaussian and Lorentzian line shapes, of almost daily necessity in ESR, are provided by **gaussian** and **lorentzian**. EasySpin also includes functions for Voigtian (convolution of Gaussian and Lorentzian, **voigtian**) and pseudo-Voigtian (linear combination of Gaussian and Lorentzian, **lshape**) line shapes.

Another convenient function, **pseumod**, emulates the effect of field modulation on a cw ESR spectrum (Hyde et al. 1990). The following Matlab lines generate the spectra shown in Figure 14, which demonstrates the influence of the modulation amplitude on the spectral line shape of a nitroxide radical:

```
Nit = struct('g', 2, 'Nucs', '14N', 'A', 40, 'lw', 0.1);
Exp = struct('mwFreq', 9.5, 'Range', [336, 343], 'Harmonic', 0);
[B, spc0] = garlic(Nit, Exp);
spc1 = pseumod(B, spc0, 0.05);
spc2 = pseumod(B, spc0, 0.4);
```

For data analysis, Savitzky-Golay smoothing filters (**smooth**) as well as polynomial and exponential fitting routines (**basecorr** and **exponfit**) are available. **rcfilt** is a digital equivalent to the common RC filter employed in cw ESR spectrometers. A set of functions (**erot**, **eulang**, **vec2ang**, **ang2vec**, **rotaxi2mat**, **rotmat2axi**) supports interconversion between rotation matrices, rotation axes and Euler angles. **sop** can be used to generate matrix representations of cartesian and shift spin operators for arbitrary spin systems.

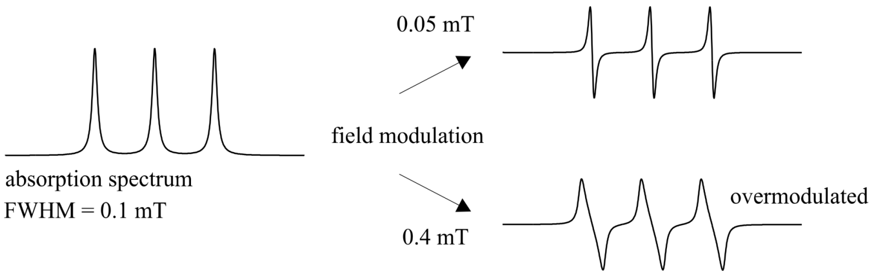

Figure 14. Effect of field modulation on a nitroxide spectrum. All simulation parameters are given in Matlab code in the text.

LIST OF EASYSPIN FUNCTIONS

General

easyspininfo	Information about EasySpin installation
eprload	Read spectrum files in common ESR data formats

Utilities

eprconvert	Graphical frequency/field/g value conversion utility
fastmotion	Fast-motion regime line widths
isotopes	A browsable list of isotopes
mhz2mt	Unit conversion from MHz to mT
mt2mhz	Unit conversion from mT to MHz

Spectral Simulations

chili	Slow-motion cw ESR spectra
garlic	Isotropic and fast-motion cw ESR spectra
pepper	Solid-state cw ESR spectra
salt	ENDOR spectra
nucfrq2d	Sketch of HYSCORE spectra

Spin Systems

nucspinadd	Adds a nucleus to a spin system
nucspinrmv	Removes a nucleus from a spin system

Data Analysis

basecorr	Polynomial baseline correction
ctafft	Cross-term averaged FFT

deriv	Numerical differentiation
exponfit	Exponential fitting
fdaxis	Frequency domain axis for FFT
pseumod	Pseudo-modulation of ESR absorption spectra
rcfilt	RC filtering of ESR spectra
smooth	Moving averages: smoothing and differentiation

Vectors, Orientations, and Angles

ang2vec	Converts polar angles to cartesian unit vector
erot	Computes rotation matrix from Euler angles
eulang	Euler angles from rotation matrix
rotaxi2mat	Convert rotation axis plus angle to rotation matrix
rotmat2axi	Convert rotation matrix to rotation axis plus angle
vec2ang	Polar angles from cartesian unit vector

Line Shapes and Windows

apowin	Apodization windows.
convspec	Convolute spectrum with line shape
gaussian	Gaussian line shape
lorentzian	Lorentzian line shape
lshape	General line shape function
makespec	Construct spectrum from peak positions and amplitudes
voigtian	Voigtian line shape function

Physical Constants

nucabund	Natural abundance of nuclear isotopes
nucdata	Nuclear spin data
nucgval	Nuclear g values
nucqmom	Nuclear electric quadrupole moments
nucspin	Nuclear spin quantum numbers
amu	Atomic unit of mass
avogadro	Avogadro constant
barn	Unit of nuclear quadrupole moments
bmagn	Bohr magneton
bohrrad	Bohr radius
boltzm	Boltzmann constant
clight	Vacuum speed of light
echarge	Elementary electric charge
emass	Mass of electron
faraday	Faraday constant
gfree	g value of the free electron
hartree	Atomic unit of energy
molgas	Molar gas constant

nmagn	Nuclear magneton
nmass	Mass of neutron
planck	Planck constant
pmass	Mass of proton
rydberg	Rydberg constant

Basic Spin Physics

commute	Commutator of two matrices
equivcouple	Coupling of equivalent spins
equivsplit	Splitting pattern for equivalent spins
hsdim	State space dimension of a spin system
larmorfrq	Larmor frequency of nuclear spins
sop	Spin operator matrices
spinvec	Spin quantum numbers in a spin system
stev	Extended Stevens operator matrices

Angular Momentum

clebschgordan	Clebsch-Gordan coefficients
plegendre	Legendre polynomials and Associated Legendre polynomials
spherharm	Spherical harmonics
wigner3j	Wigner 3-j symbols
wigner6j	Wigner 6-j symbols

Energy Levels, Resonances, and Propagations

eigfields	Resonance fields using eigenfield equation
endorfrq	ENDOR frequencies and amplitudes
evolve	Evolves density matrices in time-domain
levels	Energy levels computation
levelsplot	Energy levels and resonances plot
orisel	Orientation selection
propint	Compute pulse propagator
resfields	General resonance fields and amplitudes

Hamiltonians and Densities

eeint	Electron-electron interactions
hfine	Hyperfine interactions
internal	Internal interactions
nquad	Nuclear quadrupole interactions
sham	Full Spin Hamiltonian
sigeq	Thermal equilibrium density matrix
symm	Hamiltonian symmetry determination
zeeman	Zeeman interactions
zfield	Zero field interactions

Orientations

sphgrid	Triangular orientational grids
sphrand	Random orientational grids
sphtri	Triangulation of orientational grids

REFERENCES

Atherton NM. 1993. *Principles of electron spin resonance*. Chichester: Ellis Horwood.

Della Lunga G, Pogni R, Basosi R. 1994. Computer simulation of EPR spectra in the slow-motion regime for copper complexes with nitrogen ligands. *J Phys Chem* **98**:3937–3942.

Gamliel D, Levanon H. 1995. *Stochastic processes in magnetic resonance*. Singapore: World Scientific.

Hyde JS, Pasenkiewicz-Gierula M, Jesmanowicz A, Antholine WE. 1990. Pseudo-field modulation in EPR spectroscopy. *Appl Magn Reson* **1**:483–496.

Schneider D, Freed J. 1989. Calculating slow motional magnetic resonance spectra: a user's guide. *Biol Magn Reson* **10**:1–76.

Stoll S, A Schweiger. 2006. EasySpin, a comprehensive software package for spectral simulation and analysis in EPR. *J Magn Reson* **178**:42–55.

Stoll S, Schweiger A. 2003. An adaptive method for computing resonance fields for continuous-wave EPR spectra. *Chem Phys Lett* **380**:464–470.

Weil JA. 1971. The analysis of large hyperfine splittings in paramagnetic resonance spectroscopy. *J Magn Reson* **4**:394–399.